

Quantum and classical fidelities for Gaussian states

H. Jeong,¹ T.C. Ralph,¹ and W.P. Bowen^{2,3}

¹ Department of Physics, University of Queensland, St Lucia, Qld 4072, Australia

² Department of Physics, Faculty of Science, Australian National University, Canberra ACT 0200, Australia

³ Norman Bridge Laboratory of Physics 12-33, California Institute of Technology, Pasadena, CA 91125

(Dated: December 20, 2018)

We compare and contrast quantum and classical fidelities for Gaussian states. Their behaviors are radically different even though one is the classical limit of the other. Our investigation shows that careful analysis is necessary before any strong physical significance can be attached to quantum fidelity. This point is emphasized through a comparison with the distinguishability between quantum states achievable by some specific measurements.

I. INTRODUCTION

Quantification of the similarity (or distinguishability) of quantum states is a crucial issue in quantum information theory [1]. *Quantum fidelity* [2] - previously known as Uhlmann's transition probability [3] - is probably the most well known such quantification technique, and is an important tool for assessing the efficiency of quantum information transfer [4]. It is a direct extension of the fidelity between a pair of classical probability distributions, termed here *classical fidelity*, which is used in statistics to characterize their similarity.

Gaussian states are extremely useful tools in many quantum optics experiments. For example, several quantum communication experiments have now been performed using only Gaussian states [5, 6, 7, 8]. Typically the formulas used to calculate the quantum fidelity achieved by these experiments assume that the input states are pure coherent states [5, 6, 7, 8]. There have been many studies of quantum fidelity as a success criteria for quantum teleportation of coherent states [4, 9, 10], and its value in this regime is well understood. However, the unknown quantum states supplied by 'Victor' in real experiments are not perfectly pure, and typically have some small but non-negligible level of mixedness. This motivates us to explicitly study the quantum fidelity between mixed Gaussian states, and its usefulness for quantum information protocols.

A secondary motivation of this work was to examine the physical significance of quantum fidelity for Gaussian states. When one of the states is pure it is well known that quantum fidelity is equal to the transition probability from one state to the other; and when both states are extremely mixed, it is equal to the the classical fidelity. However, it is unclear how fidelity should be interpreted between these limits. There have been efforts to impose an operational interpretation on quantum fidelity for mixed states [11], suggest other measures with an acceptable physical interpretation [12], and compare some different distance measures [13]. Uhlmann's theorem does allow the quantum fidelity in this regime to be translated to a fidelity between higher dimensional pure states, which can then be interpreted as a transition probability between these higher dimensional states

[3]. However, the strength of the link between these hypothetical higher dimensional states and the actual states under investigation is not obvious, and remains a topic for future study.

In this paper we first investigate the relationship between quantum and classical fidelities for Gaussian states. Since Gaussian states have positive definite Wigner functions which may be interpreted as probability distributions in phase space, one might expect the quantum and classical fidelities to coincide exactly. However, this is not the case. No simple relationship can be established between quantum and classical fidelities for mixed Gaussian states even though they do coincide in the limit of the extreme mixedness. We find that mixedness, squeezing, and separation of the states involved each effect the discrepancy between classical and quantum fidelity in entirely different manners.

We also consider distinguishability by various types of measurements [14] as an alternative measure of the similarity of two quantum states. By studying the distinguishability by measurements, we demonstrate qualitatively that the discrepancies between the quantum and classical fidelities are related to the different properties of quantum and classical measurements when the two states have the same displacement in phase space. On the other hand, when the displacements are not equal the behavior of distinguishability by specific measurements does not match the quantum and classical fidelities. This suggests that quantum fidelity may not provide a good general measure of distinguishability.

This paper is organized as follows. In Section II we motivate our investigation by considering quantum teleportation of Gaussian states in an experimentally realistic regime; Section III contains derivations of expressions for quantum and classical fidelity, and compares them; in Section IV we introduce the concept of distinguishability by measurements and examine its behavior, and relationship to quantum fidelity; Section V discusses the usefulness and limitations of fidelity as a measure of the efficacy of quantum information protocols; and finally we conclude in Section VI.

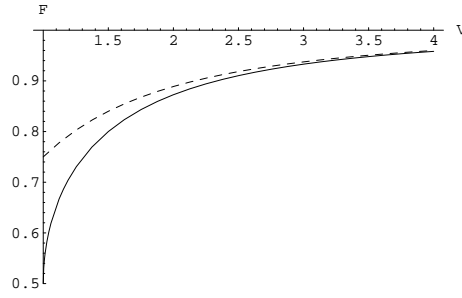


FIG. 1: The fidelity limit for quantum teleportation without entanglement against the variance of an isotropically mixed state input (solid line) and the corresponding classical fidelity (dashed line).

II. MOTIVATION

As we have noted in the introduction the unknown quantum states used in real continuous variable quantum teleportation experiments [5, 6, 7] are not exactly pure states but have some small level of mixing. A natural question is: “How sensitive is fidelity to small levels of mixing?” It is generally assumed that such a small level of mixedness will not significantly change the fidelity between the input and output states. However, as we will see here, in general this turns out not to be the case.

Let us consider the “no-entanglement” fidelity limit for unity gain quantum teleportation of coherent states. This is generally accepted to be given by a protocol in which Alice makes an ideal heterodyne measurement of the unknown state, thus obtaining an estimate of its coherent amplitude, α ; passes the measurement result to Bob who then displaces a local vacuum mode by this estimated value [5]. Bob’s state then has the same average coherent amplitude as the unknown state but its variance is increased by two units of vacuum noise. If the input state is a pure coherent state then the no-entanglement fidelity is $F_{ne} = 0.5$.

A general expression for the fidelity in this situation can easily be obtained by invoking Uhlmann’s theorem [3]. It states that if $\rho_1 = \text{Tr}_a\{|\psi_1\rangle\langle\psi_1|\}$ and $\rho_2 = \text{Tr}_a\{|\psi_2\rangle\langle\psi_2|\}$, where $|\psi_1\rangle$ and $|\psi_2\rangle$ are pure two mode states and the partial traces are only taken over one of the modes, then the fidelity of ρ_1 with respect to ρ_2 is given by

$$F_{\rho_1, \rho_2} = \max_{\psi_{1,2}} |\langle\psi_2|\psi_1\rangle|^2 \quad (1)$$

where the maximization is over all pure states which have the required reduced density operators. In our case, the reduced density operators must be those describing the input and output states, both of which are isotropically mixed coherent states. Here we limit our analysis to unity gain teleportation, in which case the average coherent amplitudes of the input and output states are equal. We can then choose $\alpha_1 = \alpha_2 = 0$ without loss of generality, and the input and output states then become thermal. In

general, to calculate the fidelity we must then maximize the fidelity over all higher dimensional states which have reduced density operators describing the required thermal states. However, it is well known that the partial trace over an EPR (2-mode squeezed) state, given by

$$|\phi_i\rangle = \frac{1}{G_i} \sum_n \left(\frac{(G_i - 1)}{G_i} \right)^{n/2} |n\rangle_a |n\rangle_b, \quad (2)$$

where $G_i \geq 1$ is the strength of the squeezing, results in a thermal state [15]. From symmetry it is clear that such a choice will maximize the fidelity as required. Thus the fidelity between two thermal states is given by

$$\begin{aligned} F &= |\langle\phi_1||\phi_2\rangle|^2 \\ &= \frac{1}{G_1 G_2} \left(\sum_n \left(\frac{(G_1 - 1)(G_2 - 1)}{G_1 G_2} \right)^{n/2} \right)^2 \\ &= \left(\frac{1}{\sqrt{G_1 G_2} - \sqrt{(G_1 - 1)(G_2 - 1)}} \right)^2 \\ &= \left(\frac{2}{\sqrt{(V_1 + 1)(V_2 + 1)} - \sqrt{(V_1 - 1)(V_2 - 1)}} \right)^2 \end{aligned} \quad (3)$$

where $V_i = 2G_i - 1$ is the variance of the single mode thermal state obtained by the partial trace of the corresponding EPR state.

We are now in a position to calculate the no-entanglement fidelity limit for teleportation of an isotropically mixed coherent state. Using Eq. (3) and the fact that the ideal heterodyne protocol discussed above adds two units of vacuum noise to the output we obtain

$$F_{ne} = \left(\frac{2}{\sqrt{(V + 1)(V + 3)} - \sqrt{(V - 1)(V + 1)}} \right)^2. \quad (4)$$

This expression is graphed as a function of the input variance $V \geq 1$ in Fig. 1. Notice that we recover $F_{ne} = 0.5$ at $V = 1$, i.e. a pure coherent state, but that the fidelity is very sensitive to small amounts of mixing. For example for 2% mixing, i.e. $V = 1.02$, a typical level of experimental purity, we have $F_{ne} = 0.57$, a 14% increase in the classical limit. Also plotted is the equivalent graph for the classical fidelity (see Eq. (13)). Notice that the quantum fidelity quite rapidly asymptotes toward the classical fidelity. This behavior motivates us to look more generally at the relationship between the quantum and classical fidelity, and to examine its physical significance.

III. COMPARISON BETWEEN QUANTUM AND CLASSICAL FIDELITIES FOR GAUSSIAN DISTRIBUTIONS

A. General expressions for fidelities of Gaussian states

Classical fidelity F_c and quantum fidelity F_q are defined as

$$F_c(P_1, P_2) = \left(\int d^2\alpha \sqrt{P_1(\alpha)P_2(\alpha)} \right)^2, \quad (5)$$

$$F_q(\rho_1, \rho_2) = \left\{ \text{Tr} \left[\sqrt{\sqrt{\rho_1}\rho_2\sqrt{\rho_1}} \right] \right\}^2, \quad (6)$$

where P_1 and P_2 are probability distributions, and ρ_1 and ρ_2 are density matrices. These density matrices can be equivalently represented as quasi-probability distributions, such as the Wigner function. The Wigner function of a general Gaussian state is

$$W(\alpha) = \frac{2}{\pi\sqrt{V^+V^-}} \exp \left[-\frac{2}{V^+}(\alpha_r \cos \phi + \alpha_i \sin \phi - \delta_r)^2 - \frac{2}{V^-}(\alpha_i \cos \phi - \alpha_r \sin \phi - \delta_i)^2 \right]. \quad (7)$$

where $V^+ = \Delta X(\phi)^2$, $V^- = \Delta P(\phi)^2$, $X(\phi) = e^{-i\phi}\hat{a} + e^{i\phi}\hat{a}^\dagger$ and $P(\phi) = -i(e^{-i\phi}\hat{a} - e^{i\phi}\hat{a}^\dagger)$. Note that the variances V^\pm are directly measurable values in experiments. Eq. (7) becomes a coherent state of amplitude δ ($= \delta_r + i\delta_i$) when $V^+ = V^- = 1$. Here the breadth of the distribution is quantified by the product V^+V^- . For quantum states this corresponds directly to the mixedness of the state, where $V^+V^- = 1$ for a pure state and $V^+V^- \rightarrow \infty$ as the mixedness increases. The level of squeezing of a Gaussian state is determined by the squeezing parameter r

$$r = \frac{1}{4}e^{i\phi} \ln \left[\frac{V^-}{V^+} \right]. \quad (8)$$

We will compare two Gaussian distributions labelled by the subscripts 1 and 2. These Gaussian distributions correspond to Wigner functions for quantum fidelity and to probability distributions for classical fidelity.

Let us first consider the case where $\delta_1 = \delta_2$, *i.e.*, the two Gaussian distributions have the same center. If we interpret the Wigner function (7) as a probability distribution, the classical fidelity between the Gaussian distributions $P_1(\alpha)$ and $P_2(\alpha)$ is straightforwardly obtained by Eq. (5) as

$$F_c = 4\sqrt{V_1^+V_1^-V_2^+V_2^-} \left\{ \cos^2 \varphi (V_1^+ + V_2^+)(V_1^- + V_2^-) + \sin^2 \varphi (V_1^+ + V_2^-)(V_1^- + V_2^+) \right\}^{-1} \quad (9)$$

where $\varphi = \phi_2 - \phi_1$ is the angle between the Gaussian distributions (see Fig. 2). The quantum fidelity between Gaussian states have been studied by some authors [17,

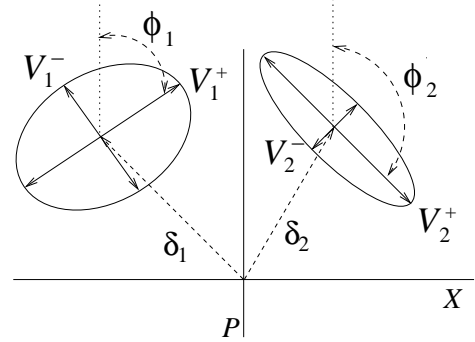


FIG. 2: Schematic of two arbitrary Gaussian distributions P_1 and P_2 .

18, 19]. It is possible to transform their formulas into more experimentally useful forms in terms of $V_{1,2}^\pm$ and φ . The quantum fidelity is found to be (see Appendix)

$$F_q = \frac{2}{\sqrt{4\sqrt{V_1^+V_2^+V_1^-V_2^-}/F_c + K - \sqrt{K}}}, \quad (10)$$

where $K = (V_1^+V_1^- - 1)(V_2^+V_2^- - 1)$. For most of the cases considered in this paper the angle φ is zero, in this case the classical and quantum fidelities are

$$F_c(\varphi = 0) = \frac{4\sqrt{V_1^+V_1^-V_2^+V_2^-}}{(V_1^+ + V_2^+)(V_1^- + V_2^-)} \quad (11)$$

$$F_q(\varphi = 0) = 2 \left\{ \sqrt{(V_1^+V_2^- + 1)(V_1^-V_2^+ + 1)} - \sqrt{K} \right\}^{-1}. \quad (12)$$

Even simpler formulas result when the amplitude and phase quadratures are symmetric ($V_1^+ = V_1^- = V_1$ and $V_2^+ = V_2^- = V_2$), in that case

$$F_c(V_1, V_2) = \frac{4V_1V_2}{(V_1 + V_2)^2} \quad (13)$$

$$F_q(V_1, V_2) = 2 \left\{ V_1V_2 + 1 - \sqrt{(V_1^2 - 1)(V_2^2 - 1)} \right\}^{-1}, \quad (14)$$

where Eq. (14) and Eq. (3) are identical.

More generally, the quantum fidelity between two distant Gaussian states with $\varphi = 0$ is (see Appendix)

$$F_q(x) = F_q(\varphi = 0)\mathcal{D}(x),$$

$$\mathcal{D}(x) = \exp \left[-\frac{2x_r^2}{V_1^+ + V_2^+} - \frac{2x_1^2}{V_1^- + V_2^-} \right], \quad (15)$$

where $x (= x_r + ix_i = \delta_2 - \delta_1)$ is the distance between the Gaussian distributions. This dependence on distance turns out to be exactly the same as one obtains for classical fidelity

$$F_c(x) = F_c(\varphi = 0)\mathcal{D}(x). \quad (16)$$

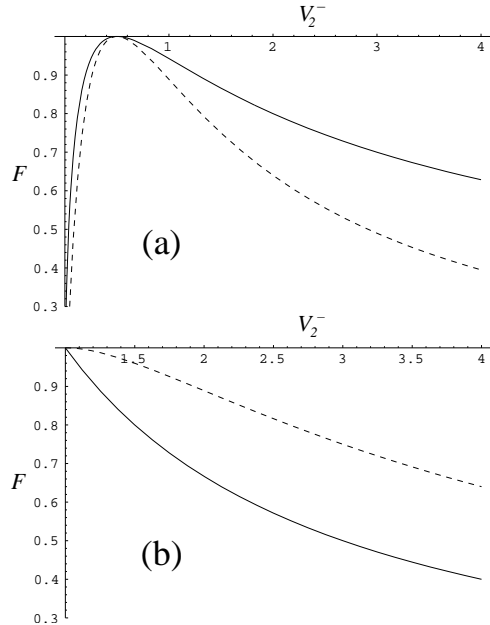


FIG. 3: Quantum (solid line) and classical (dashed line) fidelities, F , between two Gaussian distributions. (a) Both distributions pure, $V_1^+ = 2$, $V_1^- = 1/2$, $V_2^+V_2^- = 1$ and $\varphi = 0$. (b) One distribution pure, and the other mixed but with the same squeezing parameter $V_1^+ = 2$, $V_1^- = 1/2$, $V_2^+/V_2^- = 4$ and $\varphi = 0$.

B. ρ_1 or ρ_2 pure

Let us first compare F_c and F_q from Eqs. (9) and (10) when one of the states is pure. In this case, a simple relationship can be drawn between the quantum and classical fidelities

$$F_q^2 = \frac{F_c}{\sqrt{V_2^+V_2^-}}. \quad (17)$$

Here, as in all following cases, when comparing classical and quantum fidelities the properties of distribution 1 are fixed while those of distribution 2 are varied. The quantum and classical fidelities between two distributions with $V_1^+ = 2$, $V_1^- = 1/2$, $V_2^+V_2^- = 1$ and $\varphi = 0$ are compared in Fig. 3(a). For quantum fidelity, this condition corresponds to two pure quantum states, one of which has a varying degree of squeezing while the other has a fixed squeezing parameter of $r = -0.347$. We see that classical fidelity degrades faster than quantum fidelity. This result can be obtained straightforwardly from Eq. (17). We see that when $V_2^+V_2^- = 1$, $F_c = F_q^2$; remembering the bound on fidelity $0 \leq \{F_c, F_q\} \leq 1$ it is clear that $F_c \leq F_q$.

Let us now consider the quantum and classical fidelities between a pure squeezed state, and a mixed state with the same squeezing parameter. Results for the parameters $V_1^+ = 2$, $V_1^- = 1/2$, $V_2^+/V_2^- = 4$, $r = -0.347$, and $\varphi = 0$ are shown in Fig. 3(b). We see that the quantum fidelity degrades faster than the classical fidelity as the difference in the mixedness of the two states increases.

This trend directly contrasts that obtained in Fig. 3(a) as the discrepancy in the squeezing parameters of the two states increases.

The results in Fig. 3(b) seem to reflect the difference between quantum and classical distributions with respect to mixedness. Since a classical ensemble consists simply of a mixture of classical states each weighted by the distribution function, it is essentially entirely mixed regardless of the breadth of the distribution. A quantum state however, is perfectly pure if the breadth is unity ($V_+V_- = 1$), and the mixedness increases as $V_+V_- \rightarrow \infty$. So, increasing the breadth of the distribution has a secondary effect for quantum states which is not present for classical distributions. It is reasonable, then, that differences in breadth cause a greater reduction in the similarity (and hence fidelity) of quantum states than that of their classical counterparts under the same conditions.

C. ρ_1 and ρ_2 mixed

As we have explained in Sec. II, it may not be acceptable to simply assume that the input state is pure in real teleportation experiments, since the quantum fidelity can be extremely sensitive to even small amounts of mixedness. For example, the quantum fidelity between a coherent state of $V_1 = 1$ and a thermal state of $V_2 = 2$ is $F \approx 0.667$, whereas for thermal states with $V_1 = 1.05$ and $V_2 = 2$ ($V_1 = 1.01$ and $V_2 = 2$) it is $F \approx 0.785$ ($F \approx 0.721$). If a pure input state was assumed for the latter cases the fidelity would be only $F \approx 0.667$, a significantly underestimation.

In Fig. 4, the breadth of the distributions are four times larger than those for the previous case (Fig. 3), while all the other conditions are same. The same trends to those in Fig. 3 are observed but the differences between quantum and classical fidelities are smaller. In other words, the discrepancy between quantum and classical fidelity is reduced as the breadth (V^+V^-) of the Gaussian distributions increases. The two fidelities become identical as $V_1^+V_1^- \rightarrow \infty$ and $V_2^+V_2^- \rightarrow \infty$. Since in this limit the quantum states can be treated as classical objects we see that the classical limit of quantum fidelity is classical fidelity as expected.

As a final example, let us consider the effect of rotating one distribution in phase space. Suppose the two Gaussian distributions have the same absolute squeezing parameter, ($V_1^+/V_1^- = V_2^+/V_2^- = 16$, $|r| = 0.693$), but different breadths ($V_1^+V_1^- = V_2^+V_2^-/4 = 1$), and are initially aligned ($\varphi = 0$). In this case, as was seen previously, the difference in breadth causes the classical fidelity to be greater than the quantum fidelity (similar to Fig. 3(b)). However, if one begins to change the relative angle φ between the distributions, the squeezing parameters, r_1 and r_2 , of the distributions become different. At a certain point, this difference may become more dominant than the difference in breadth (similar to Fig. 3(a)). Thus the difference between quantum and classical fidelities

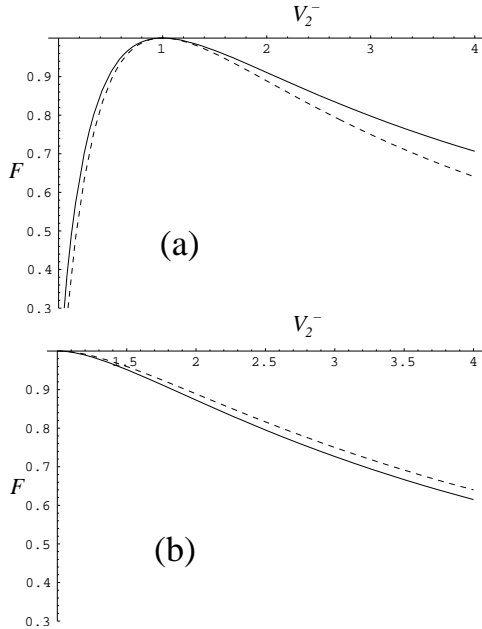


FIG. 4: Quantum (solid line) and classical (dashed line) fidelities between Gaussian distributions. (a) $V_1^+ = 4$, $V_1^- = 1$, $V_2^+V_2^- = 4$ and $\varphi = 0$. (b) $V_1^+ = 4$, $V_1^- = 1$, $V_2^+/V_2^- = 4$ and $\varphi = 0$. The breadths of the Gaussian distributions are four times larger than those in Fig. 3.

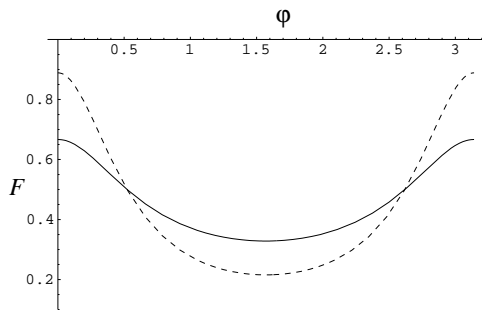


FIG. 5: Quantum (solid line) and classical (dashed line) fidelities for two Gaussian distributions having the same absolute squeezing parameter, $V_1^+/V_1^- = V_2^+/V_2^- = 16$ ($|r| = 0.693$), yet different breadths $V_1^+V_1^- = V_2^+V_2^-/4 = 1$. The Quantum and classical fidelities vary differently with the relative angle.

ties gets smaller and eventually classical fidelity becomes greater as shown in Fig. 5.

In the previous discussion in this Section, we have considered the cases of which the Gaussian distributions have the same center. The distance between Gaussian distributions in phase space is another factor which degrades fidelity. In Sec. III A, we pointed out that the exponential factors, which characterize effects of a distance in phase space, in quantum and classical fidelities are exactly the same. This means that distance between the Gaussian distributions in phase space does not result in any discrepancy between quantum and classical fidelities.

IV. DISTINGUISHABILITY OF GAUSSIAN STATES BY QUANTUM AND CLASSICAL MEASUREMENTS

In this Section we investigate the distinguishability of Gaussian distributions through quantum and classical measurements. In a classical system, all observables commute so that simultaneous perfect measurements are possible. In a quantum system this is clearly not allowed, however techniques that measure quanta, such as photon counting, become available that can enhance the measurement outcomes in some circumstances. We attempt this complementary approach to clarify some of the discrepancies between quantum and classical fidelities.

A. Fidelity and distinguishability by specific measurements

If fidelity is a good measure of distinguishability, it may be conjectured that the quantum and classical fidelities should be consistent with distinguishability by quantum and classical measurements. I.e., if quantum fidelity is larger than classical fidelity for two given states, the distinguishability between those states by a quantum measurement should be lower than the distinguishability by a classical measurement. Such distinguishability can be dependent on the specific type of measurement performed. In optics experiments, photon detection, which resolves individual photons, is considered a typical quantum measurement. On the other hand, homodyne detection can be considered a classical measurement: it does not resolve individual quanta, and distinguishability between two Gaussian states by ideal homodyne detection does not depend on the absolute size of the distributions but only on their relative widths. However, homodyne detection still measures only one of the quadrature variables. In the classical limit, homodyne measurements can be performed for both quadrature variables simultaneously. Such perfect dual-homodyne measurements can be approximated by a beam splitter and two homodyne measurement settings only when both of the Gaussian states are extremely mixed. In this section, we relate photon detection, homodyne detection and dual-homodyne detection to quantum, semi-classical and classical measurements respectively, and investigate the distinguishability that can be achieved by each.

Distinguishability between two states $|\psi_1\rangle$ and $|\psi_2\rangle$ can be defined as the probability of correctly discriminating between the states by a generalized measurement of which the measurement elements are $\{\hat{\pi}_k\}$. We assume that no measurement results are abandoned to guess the unknown given state, *i.e.*,

$$\hat{\pi}_1 + \hat{\pi}_2 = \mathbb{1} \quad (18)$$

where $|\psi_1\rangle$ ($|\psi_2\rangle$) is discerned by $\hat{\pi}_1$ ($\hat{\pi}_2$). If the states $|\psi_1\rangle$ and $|\psi_2\rangle$ are given with equal probability, distin-

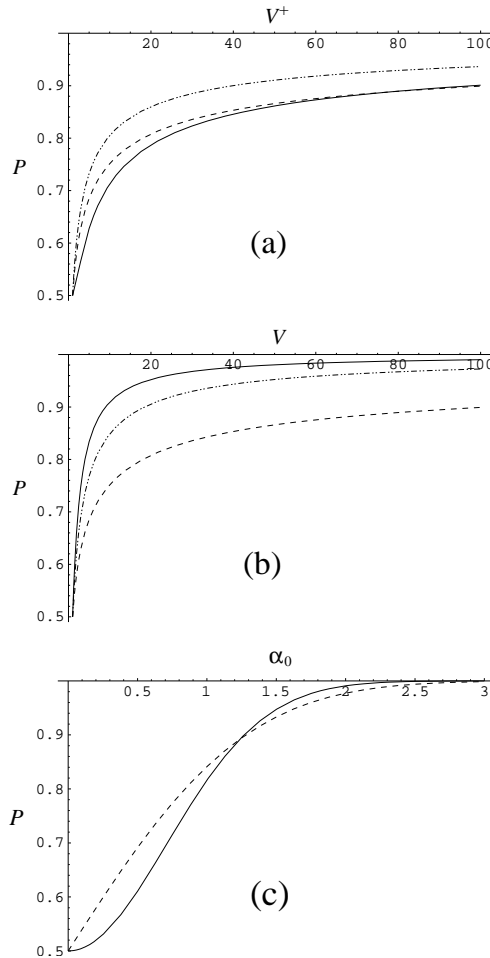


FIG. 6: Distinguishability P by photon detection (solid line), homodyne detection (dashed line) and dual-homodyne detection (dotted line). (a) A vacuum state and a pure squeezed state with anti-squeezed quadrature variance V^+ , (b) a vacuum state and a thermal state with amplitude and phase quadrature variances of V , and (c) a vacuum state and a coherent state with coherent amplitude α_0 . The distinguishability by homodyne and dual-homodyne detection are identical for (c).

guishability is [14]

$$P = \frac{1}{2}(\langle \psi_1 | \hat{\pi}_1 | \psi_1 \rangle + \langle \psi_2 | \hat{\pi}_2 | \psi_2 \rangle), \quad (19)$$

which can be generalized for two mixed states ρ_1 and ρ_2 :

$$P = \frac{1}{2}(\text{Tr}[\rho_1 \hat{\pi}_1] + \text{Tr}[\rho_2 \hat{\pi}_2]). \quad (20)$$

B. ρ_1 or ρ_2 pure

Suppose first that our aim is to distinguish a vacuum state $|\psi_1\rangle = |0\rangle$ from a pure squeezed vacuum state

$|\psi_2\rangle = |S_0\rangle$ with squeezing parameter $r(V^+, V^-; \phi = 0)$ where $V^+ > V^-$, through photon detection, homodyne detection, or dual-homodyne detection. Since a vacuum state contains no photon, the elements of “quantum” measurement should be

$$\hat{\pi}_{q1} = |0\rangle\langle 0|, \quad \hat{\pi}_{q2} = \sum_{k=1}^{\infty} |k\rangle\langle k|, \quad (21)$$

where $|k\rangle$ ’s are number states. The distinguishability by photon detection can then be calculated from Eqs. (18), (19) and (21) as

$$P_q = 1 - \left(V_+ + \frac{1}{V_+} + 2 \right)^{-\frac{1}{2}} \quad (22)$$

The elements of “semi-classical” measurement need to be assigned as

$$\hat{\pi}_{c1}(|x| \leq x_0) = \int_{|x| \leq x_0} dx |x\rangle\langle x|, \quad (23)$$

$$\hat{\pi}_{c2}(|x| > x_0) = \int_{|x| > x_0} dx |x\rangle\langle x|, \quad (24)$$

$$x_0 = \frac{1}{2} \sqrt{\frac{V^+ \ln[V^+]}{(V^+ - 1)}}, \quad (25)$$

where the Wigner function $W_2(\alpha_r = x; \alpha_i = 0)$ of the squeezed state $|S_0\rangle$ is larger than $W_1(\alpha_r = x; \alpha_i = 0)$ of the vacuum $|0\rangle$ for $|x| > x_0$. The distinguishability by homodyne detection is then

$$\begin{aligned} P_{hd} &= \frac{1}{\sqrt{2\pi}} \left\{ 2 \int_0^{x_0} dx e^{-2x^2} + 2 \int_{x_0}^{\infty} dx \frac{e^{-\frac{2x^2}{V^+}}}{\sqrt{V^+}} \right\} \\ &= \frac{1}{2} (\text{Erf}[\sqrt{2}x_0] + \text{Erfc}[\frac{\sqrt{2}x_0}{\sqrt{V^+}}]). \end{aligned} \quad (26)$$

The distinguishability by perfect dual-homodyne detection is obtained by extending Eq. (26) as

$$P_c = \frac{1}{2\pi} \left\{ \int_{\mathcal{A}} dx dy e^{-2(x^2 + y^2)} + \int_{\mathcal{B}} dx dy e^{-2(\frac{x^2}{V^+} + V^+ y^2)} \right\}, \quad (27)$$

where \mathcal{A} is the region in which the Wigner function $W_1(\alpha_r = x; \alpha_i = y)$ of the vacuum is larger than the Wigner function $W_2(\alpha_r = x; \alpha_i = y)$ of the squeezed state while \mathcal{B} is the complementary set of \mathcal{A} . We note again that dual-homodyne measurements are possible only for two classical distributions (or for extremely mixed Gaussian quantum states). Eq. (27) can be solved using numerical techniques. The results for distinguishability by photon detection, homodyne detection and dual-homodyne detection are plotted in Fig. 6(a). The distinguishability achieved by homodyne detection is higher than that by photon detection up to $V^+ < 77.6$, and the distinguishability by photon detection becomes slightly higher thereafter. The distinguishability by dual-homodyne detection is always better than that by photon

detection. This is in agreement with the result seen earlier that quantum fidelity is always higher than classical fidelity for two pure states.

Now consider a pure vacuum and a thermal state of variance $V^+ = V^- = V$. In this case, the distinguishability by the quantum measurement described in Eq. (21) is

$$P_q = \frac{V}{V+1}. \quad (28)$$

The distinguishability by homodyne detection P_{hd} can be obtained by substituting V^+ with V in Eqs. (25) and (26); and the distinguishability by dual-homodyne detection is

$$P_c = \frac{1}{2\pi} \left\{ \int_{\mathcal{A}'} dx dy e^{-2(x^2+y^2)} + \int_{\mathcal{B}'} dx dy \frac{e^{-\frac{2(x^2+y^2)}{V}}}{\sqrt{V}} \right\}, \quad (29)$$

where \mathcal{A}' is the region in which the Wigner function $W_1(\alpha_r = x; \alpha_i = y)$ of the vacuum is larger than the Wigner function $W_2(\alpha_r = x; \alpha_i = y)$ of the thermal state, while \mathcal{B}' is the complementary set of \mathcal{A}' . Eq. (29) can be integrated using the cylindrical coordinate with the result that

$$P_c = \frac{1}{2} (1 + V^{\frac{1}{1-V}} - V^{\frac{V}{1-V}}). \quad (30)$$

Fig. 6(b) compares these three distinguishabilities, we see that photon detection can distinguish between thermal states significantly better than both homodyne and dual-homodyne detection. This is in good agreement with the result that classical fidelity is always higher than quantum fidelity in this case.

As with the quantum and classical fidelities in Section III, let us now consider two distant coherent states. If the two coherent states are $|0\rangle$ (vacuum) and $|\alpha_0\rangle$, the “classical” measurement elements are $\pi_{c1}(x \geq \alpha_0/2)$ and $\pi_{c2}(x < \alpha_0/2)$ and the quantum measurement elements are the same as in Eq. (21). In this case, the distinguishability by homodyne and dual-homodyne detection are identical as no additional information is provided by measuring the quadrature orthogonal to α_0 . The distinguishability by photon and homodyne (or dual-homodyne) detection are then

$$P_q = 1 - \frac{e^{-\alpha_0^2}}{2}, \quad (31)$$

$$P_{hd} = P_c = \frac{1}{2} (1 + \text{Erf}[\frac{\alpha_0}{\sqrt{2}}]). \quad (32)$$

One would expect the distinguishabilities P_q and P_c in Eqs. (31) and (32) to be the same, to agree with the result for quantum and classical fidelities. However, we observe that distinguishability by homodyne (or dual-homodyne) detection is higher for $x < 1.24$ but distinguishability by photon detection is higher for $x > 1.24$ as shown in Fig. 6.

It is worth noting that the relation between quantum fidelity F_q and distinguishability P_q by photon detection

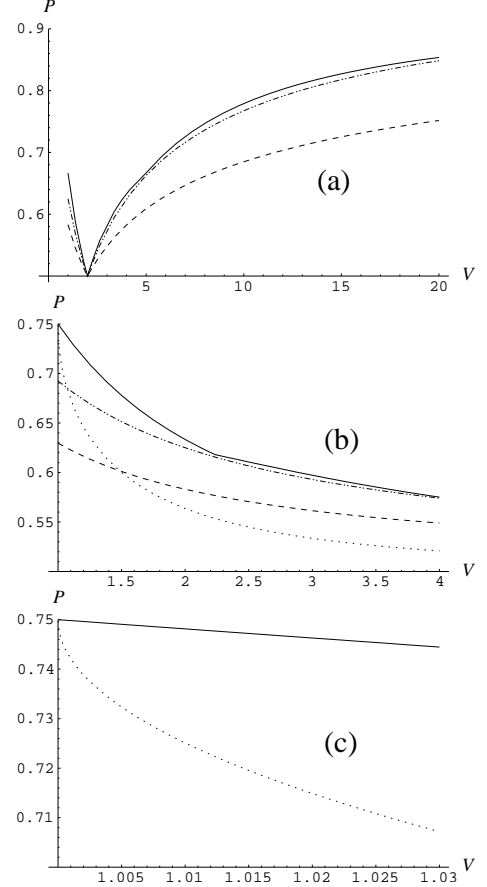


FIG. 7: (a) Distinguishability P by photon detection (solid line), homodyne detection (dashed line) and dual-homodyne detection (dotted line) between two thermal states with variances of V and 2 , respectively. (b) Distinguishability by photon detection (solid line), homodyne detection (dotted line), dual-homodyne detection (dotted line), and inferred distinguishability by quantum fidelity, $P = 1 - F_q/2$ (dot-dashed line). Two thermal states with variances of V and $V + 2$ are compared, this corresponds to the “no-entanglement” teleportation limit. (c) Same as (b) but with finer scale on the horizontal axis. The distinguishability by photon detection does not show the same radical degradation as quantum fidelity.

$$P_q = 1 - \frac{F_q}{2} \quad (33)$$

always holds in Eqs. (22), (28) and (31). This implies that quantum fidelity may be monotonically related to distinguishability by a specific quantum measurement at least when one of the states is pure.

C. ρ_1 and ρ_2 mixed

Let us now generalize the results shown in Fig. 6(b) to two isotropically mixed states of variances V_1 and V_2

in line with our original motivation discussed in Sec. II. The distinguishability by photon detection for two mixed thermal states can be straightforwardly obtained by the same method used above as

$$P_q = \frac{1}{2} \left\{ 1 - \left(\frac{V_1 - 1}{V_1 + 1} \right)^{1+k_0} + \left(\frac{V_2 - 1}{V_2 + 1} \right)^{1+k_0} \right\}, \quad (34)$$

$$k'_0 = \frac{\ln[(V_2 + 1)/(V_1 + 1)]}{\ln[(V_2 - 1)/(V_2 + 1)] - \ln[(V_1 - 1)/(V_1 + 1)]},$$

where $V_2 > V_1$ and k_0 is the largest integer smaller than k'_0 . The integer k_0 is the threshold of the discrimination. For example, k_0 is 1 for $V_1 = 3$ and $V_2 = 4$, and in this case, the state ‘2’ is reckoned to be measured when the outcome of the photon detection is larger than 1. Eq. (34) is reduced to Eq. (28) for $V_1 = 1$, *i.e.*, when one of the states is the pure vacuum. Note that the relation (33) between distinguishability by photon detection and quantum fidelity does not hold when both of the states are mixed. Distinguishability by homodyne detection is

$$P_{hd} = \frac{1}{2} (\text{Erf}[\frac{\sqrt{2}\bar{x}_0}{\sqrt{V_1}}] + \text{Erfc}[\frac{\sqrt{2}\bar{x}_0}{\sqrt{V_2}}]), \quad (35)$$

$$\bar{x}_0 = \frac{1}{2} \sqrt{\frac{V_1 V_2 \ln[V_2/V_1]}{(V_2 - V_1)}}.$$

The distinguishability by dual-homodyne detection is

$$P_c = \frac{1}{2} \left\{ 1 + \left(\frac{V_2}{V_1} \right)^{\left(\frac{V_1}{V_1 - V_2} \right)} - \left(\frac{V_2}{V_1} \right)^{\left(\frac{V_2}{V_1 - V_2} \right)} \right\}, \quad (36)$$

which can be obtained by the same method used for Eq. (29). The distinguishability by ‘quantum’ and ‘classical’ measurements P_q and P_c become identical when the Gaussian states are extremely mixed as shown in Fig. 7(a). It is also found from Eq. (34) that distinguishability by photon detection is much less sensitive to mixedness of Gaussian states than quantum fidelity. For example, distinguishability by photon detection between a coherent state of $V_1 = 1$ and a thermal state of $V_2 = 3$ is $P_q \approx 0.75$, and it is $P_q \approx 0.746$ for thermal states of $V_1 = 1.02$ and $V_2 = 3.02$. Such a moderate change is in sharp contrast with the radical increase of quantum fidelity for the same cases explained in Sec. II. This contrast is evident in Figs. 7(b) and 7(c), where distinguishability by photon detection, homodyne detection, dual homodyne detection, and distinguishability inferred by quantum fidelity from Eq. (33), $P = 1 - F_q/2$, have been plotted. In Figs. 7(b) and 7(c), two thermal states with variances V and $V + 2$ have been compared, which corresponds to the ‘no-entanglement’ teleportation limit. The results discussed above in this Section raises doubts about quantum fidelity as a good general measure of distinguishability.

V. FIDELITY FOR QUANTUM INFORMATION PROTOCOLS

One of the most common applications of quantum fidelity is to measure the efficacy of quantum information protocols [1]. Typically, to characterize such protocols one begins with an ensemble of identical known input states. The protocol is then performed on each input state, yielding an ensemble of (hopefully identical) output states. These states can be fully characterized by performing tomographic measurements. The desired output state [20] from the protocol is typically well known, for example in unity gain quantum teleportation it would simply be the input state. The fidelity between this desired output state and the actual output state can then be directly calculated, and is used to judge the efficacy of the protocol. However, we have seen that fidelity is highly sensitive to both squeezing of, and impurity in, the states being compared. Furthermore, when both states are impure, it is difficult to attribute anything more than a weak physical significance to fidelity. Since in any realistic experiment all states involved (except perhaps vacuum states) will be at least somewhat impure, the usefulness of fidelity per se as a measure of the efficacy of quantum information protocols is questionable. Furthermore, since the fidelity of a quantum information protocol depends strongly on the properties of the input state, care must be taken when using fidelity to make comparisons between even very similar experiments.

At this point one would be forgiven for contemplating rejecting fidelity entirely as an efficacy measure. However, it does have one very attractive feature: when at least one of the states involved is pure, it is simply the transition probability between the two states. In other words, if one was to make a projective measurement on the output state, fidelity is the probability that it would collapse into the desired output state. Also, as we have seen, there is a consistent relationship between distinguishability and fidelity if one state is pure. These make fidelity a useful figure of merit, but to apply it to a quantum information protocol the desired output state must be pure. This is very difficult to ensure in practice. An alternative technique, that we advocate here, is to characterize the transfer function of the quantum information protocol. In general, this will involve characterizing the function that maps the Wigner function of the input state to that of the output state. The fidelity for any arbitrary input state can then be calculated simply by applying the transfer function, and then comparing the resulting predicted output state to the desired output state. The fidelity for some *reference input state*, which can be chosen arbitrarily, can then be calculated. Fidelity calculated in this way has the following advantages: 1) since a pure input state can be chosen, the desired output state from the protocol will also often be pure [21], the fidelity obtained then has physical significance as the transition probability between the desired and predicted output states; and 2) since the same reference input state can be used for

all experimental implementations of quantum information protocols, this fidelity can be used as a benchmark to compare efficacies.

A. Quantum teleportation as an example

Let us consider, for example, how this process would work for unity gain continuous variable quantum teleportation. As mentioned above, the desired output for unity gain continuous variable quantum teleportation is the input state. However, as a result of imperfect entanglement and technical noise sources the actual output state will be somewhat degraded. This effect is quantified by the transfer function of the system; defined by the gain of the process which due to experimental imperfections will not be exactly unity [6], and the additional noise present on the output state over-and-above the noise present on the input state. In general the additional noise is non-Gaussian and tomographic techniques are required for a full characterization, however when Gaussian entanglement is used and all other noise sources are Gaussian only the variance of the noise is required [6, 16]. This is the case for all continuous variable teleportation experiments to date [5, 6, 7]. Once the gain and noise variance have been determined an arbitrary reference input state can be chosen and the corresponding output state calculated. A sensible choice of reference input state in this case would be a coherent state, since the classical fidelity limit for teleportation is normally quoted for coherent states. The fidelity between this reference coherent state and the output state can be directly calculated, and used to compare different teleportation experiments. As we saw in Fig. 1, if this transfer function and reference state technique is not used to characterize teleportation experiments, the fidelities quoted by different experiments will vary significantly based on variations in the mixedness of the input states. This variation has no bearing on the strength of entanglement used in the experiment, or the efficacy of the protocol. Note that in most teleportation experiments to date it has simply been assumed their input states were pure without justification. For small levels of mixedness, this is approximately (but not exactly) equivalent to what we suggest here.

VI. REMARKS

In this paper we have investigated the quantum fidelity between Gaussian states. Investigations of this kind are important, since all continuous variable quantum information experiments to date have been performed with such states. The input states in these experiments are normally treated as pure coherent states [5, 6, 7]. However, small levels of mixedness are typically present. We

find that even these levels of mixedness significantly alter the quantum fidelity. Hence, it is typically not appropriate to simply assume that the input states are pure. In an attempt to understand why quantum fidelity is so sensitive to mixedness, and to gather some understanding of its physical significance between two mixed states, we consider its classical counterpart, the classical fidelity between two probability distributions. Since the Wigner functions of Gaussian states are positive definite, one might expect the quantum and classical fidelities to be identical. We find, however that they show radically different behaviors. Classical fidelity between probability distributions is degraded more strongly than quantum fidelity between quantum states as a result of differences in squeezing parameters. On the other hand, the quantum fidelity degrades faster than the classical fidelity as the breadth ($\Delta X^2 \Delta P^2$) of the distributions diverge. The distance between two Gaussian states in phase space does not cause any discrepancy between the quantum and classical fidelities.

Fidelity in both the classical and quantum regimes is touted as a measure of distinguishability. To understand the differences between quantum and classical fidelity we calculate the distinguishability achieved by some specific measurements in the two regimes. Since different measurement types are available in quantum and classical regimes, it is perhaps unsurprising that radical difference in both the distinguishability and fidelity can exist. We find that the distinguishability and fidelity show the same qualitative behavior as a result of differences in the distribution breadths and squeezing parameters. However, distinguishability by specific measurements and fidelity show qualitatively different behavior as a function of the distance in phase space between the two distributions. It should be noted that a full characterization of the distinguishability between two states requires an analysis of all possible measurements on the states. Such an analysis was not attempted here.

Although, a clear physical significance can be attached to quantum fidelity when one of the states involved is pure, our results indicate that when both states are mixed, quantum fidelity loses this significance. For this reason, we propose the use of transfer functions to characterize continuous variable quantum information protocols. Once the transfer function of the protocol is determined, the fidelity that would be achieved between an arbitrary pure input state, and the output state can be calculated. The resulting value has physical significance and can be used as a benchmark to compare between experiments.

This work was supported by the Australian Research Council. WPB acknowledges financial support from the Center for the Physics of Information, California Institute of Technology.

[1] M.A. Nielsen and I.L. Chuang, *Quantum computation and quantum information* (Cambridge, 2000).

[2] R. Jozsa, *J.Mod.Opt.*, **41**, 2315 (1994).

[3] A. Uhlmann, *Rep.Math.Phys.* **9**, 273 (1976).

[4] S.L. Braunstein, C.A. Fuchs and H.J. Kimble, *J. Mod. Opt.* **9**, 273 (1976)

[5] A. Furusawa, J.L. Sorensen, S.L. Braunstein, C.A. Fuchs, H.J. Kimble and E.S. Polzik, *Science* **282** 706 (1998).

[6] W.P. Bowen, N. Treps, B.C. Buchler, R. Schnabel, T.C. Ralph, H.-A. Bachor, T. Symul, P.K. Lam, *Phys. Rev. A* **67**, 032302 (2003); W.P. Bowen, N. Treps, B.C. Buchler, R. Schnabel, T.C. Ralph, T. Symul, P.K. Lam, *IEEE J.S.T.Q.E.* **9**, 1519 (2003).

[7] T.C. Zhang, K.W. Goh, C.W. Chou, P. Lodahl, and H.J. Kimble, *Phys. Rev. A* **67**, 033802 (2003)

[8] A. Lance, T. Symul, W. P. Bowen, B. C. Sanders, and P. K. Lam, *Phys.Rev.Lett.* **92**, 177903 (2004).

[9] F. Grosshans and P. Grangier, *Phys.Rev.A* **64**, 010301(R) (2001); S.L. Braunstein, C.A. Fuchs, H.J. Kimble, P. van Loock, *Phys. Rev. A* **64**, 022321.

[10] C.M. Caves, K. Wódkiewicz, *quant-ph/0409063*.

[11] J.L. Dodd and M.A. Nielsen, *Phys.Rev.A* **66**, 044301 (2002).

[12] J. Lee, M.S. Kim, and Č. Brukner, *Phys.Rev.Lett* **91**, 087902 (2003).

[13] A. Gilchrist, N.K. Langford, and M.A. Nielsen, *quant-ph/0408063*.

[14] C.A. Fuchs, Ph.D. thesis, University of New Mexico (1995); S.M. Barnett, C.R. Gilson, Masahide Sasaki, *J. Phys. A: Math. Gen.* **34**, 6755 (2001).

[15] D.F. Walls and G.J. Milburn, *Quantum Optics*, Springer-Verlag (1994).

[16] T.C.Ralph and P.K.Lam, *Phys.Rev.Lett.*, **81**, 5668 (1998).

[17] J. Twamley, *J.Phys.A* **29**, 3723 (1996).

[18] X.- B. Wang, C.H. Oh, and L.C. Kwek, *Phys.Rev.A* **58**, 4186 (1998).

[19] Gh.- S. Paraoanu and H. Scutaru, *Phys.Rev.A* **58**, 869 (1998).

[20] That is, the output state that would be achieved if the protocol ran perfectly.

[21] There are some exceptions, such as non-unity gain teleportation.

APPENDIX A: QUANTUM FIDELITY FOR GAUSSIAN STATES

The density matrix of a general Gaussian state can be expressed as

$$\rho = Z(\beta)D(x)S(r)\exp[-\frac{\beta}{2}(aa^\dagger + a^\dagger a)]S^\dagger(r)D^\dagger(x), \quad (A1)$$

where $S(r)$ is the squeezing operator, $D(x)$ is the displacement operator, and $Z(\beta)$ is the normalization factor. Quantum fidelity between two Gaussian states ρ_1 and ρ_2 , for $x_1 = x_2$, is then [17]

$$F_q^{(\varphi)} = \frac{2 \sinh \frac{\beta_1}{2} \sinh \frac{\beta_2}{2}}{\sqrt{Y} - 1} \quad (A2)$$

where

$$Y = \cos^2 \varphi \left[\cosh^2(r_2 - r_1) \cosh^2 \frac{(\beta_1 + \beta_2)}{2} - \sinh^2(r_1 - r_2) \cosh^2 \frac{(\beta_2 - \beta_1)}{2} \right] + \sin \varphi \left[\cosh^2(r_1 + r_2) \cosh^2 \frac{(\beta_1 + \beta_2)}{2} - \sinh^2(r_1 + r_2) \cosh^2 \frac{(\beta_2 - \beta_1)}{2} \right]. \quad (A3)$$

The variances V^\pm for a Gaussian state of the general form (A1) are

$$V^+ = \Delta X^2 = 1 + A + B, \quad (A4)$$

$$V^- = \Delta P^2 = 1 + A - B, \quad (A5)$$

$$A = 2[\bar{n} + (2\bar{n} + 1) \sinh^2 r], \quad (A6)$$

$$B = 2(2\bar{n} + 1) \cosh \phi \sinh r \cosh r, \quad (A7)$$

$$\bar{n} = \text{Tr}[\rho \hat{a}^\dagger \hat{a}] = \frac{1}{e^\beta - 1}, \quad (A8)$$

where \bar{n} corresponds to the average photon number. Then the squeezing parameter r and inverse temperature

β can be expressed in terms of $V_{1,2}^\pm$ and φ as

$$\beta = \ln[1 + \frac{2}{\sqrt{V^+ V^- - 1}}], \quad (A9)$$

and Eq. (8). Eq. (10) is obtained from Eqs. (8), (A9), (A2) and (A3).

Quantum fidelity between two distant Gaussian states ρ_1 and ρ_2 , for $\varphi = 0$, was calculated by Wang *et al.* [18] as

$$F_q^{(x)} = F_q^{(\varphi=0)} \mathcal{D}, \quad (A10)$$

where

$$\begin{aligned}\mathcal{D} &= \exp\left[\frac{(\epsilon_1 + \epsilon_2)}{\Delta}\right], \\ \Delta &= \cosh \beta_1 \cosh \beta_2 + \sinh \beta_1 \sinh \beta_2 \cosh 2(r_1 - r_2) - 1, \\ \epsilon_1 &= \sinh \beta_1 \sinh^2 \frac{\beta_2}{2} \left[(g^2 + g^{*2}) \sinh 2r_1 - 2|g|^2 \cosh 2r_1 \right], \\ \epsilon_2 &= \sinh \beta_2 \sinh^2 \frac{\beta_1}{2} \left[(g^2 + g^{*2}) \sinh 2r_2 - 2|g|^2 \cosh 2r_2 \right].\end{aligned}\quad (\text{A11})$$

By substituting β and r in Eqs. (A10) and (A11) with Eqs. (A9) and (8), Eq. (15) is obtained.